

[2015]This manuscript version is made available under the CC-BY-NC-ND 4.0 license <http://creativecommons.org/licenses/by-nc-nd/4.0/>  
This document is the Accepted Manuscript version of a Published Work that appeared in final form in Engineering Geology. To access the final edited and published work see [10.1016/j.enggeo.2015.08.008]

## Abandoned mine tailings in cultural itineraries: Don Quixote Route (Spain)

Tomás Martín-Crespo<sup>a</sup>, \*, David Gómez-Ortiz<sup>a</sup>, Silvia Martín-Velázquez<sup>a</sup>, José María Esbrí<sup>b</sup>, Cristina de Ignacio-San José<sup>c</sup>, María José Sánchez-García<sup>d</sup>, Isabel Montoya-Montes<sup>e</sup>, Fidel Martín-González<sup>a</sup>

**a** Dpto. Biología y Geología, Física y Química Inorgánica, ESCET, Universidad Rey Juan Carlos, C/Tulipán s/n, 28933 Móstoles, Madrid Spain

**b** Instituto de Geología Aplicada (IGeA), Escuela de Ingeniería Minera e Industrial de Almadén (UCLM), Plaza Manuel Meca, 1. 13.400 Almadén, Ciudad Real, Spain

**c** Dpto. Petrología y Geoquímica, Fac. CC. Geológicas, Universidad Complutense de Madrid, C/Antonio Novais s/n, 28040 Madrid, Spain

**d** Dpto. Física, Facultad CC. del Mar, Universidad de las Palmas de Gran Canaria, C/Juan de Quesada, 30, 35001, Las Palmas de Gran Canaria Spain

**e** Dpto. Oceanografía Física, Química y Geológica, Instituto Oceanográfico, Universidad de São Paulo, Praça do Oceanográfico, 191, 05508-120, São Paulo, Brasil

\* Corresponding author.

### Abstract

Metallic mining wastes are a crucial environmental concern because of the accumulation and emission of toxic elements. The abandoned San Quintín mine tailings, from the exploitation of galena and sphalerite (Puertollano mining district, Spain), are surrounded by farmland and are crossed by the European Cultural Itinerary known as the "Don Quixote Route". Geophysical, mineralogical and geochemical techniques have been applied to determine the geometry and composition of mine ponds and the possible occurrence of AMD that could entail ecosystem and human risks. Seven electrical resistivity tomography profiles were surveyed, and re-worked tailing samples of two ponds, five soil samples, nine water samples and gaseous mercury emissions were analyzed. Both mine ponds are ~ 8 m deep and overlie Quaternary colluvial sediments deposited over Precambrian metasediments. The pond infilling is mainly composed of quartz and clay minerals, and minor amounts of gypsum and sulfides, with significant As, Cd, Hg, Pb, Sb and Zn contents. This metal emission source affects the underlying colluvial sediments and high Hg and Pb contents have also been found in nearby agricultural soils. AMD has been identified, but metal contamination in the stream that borders the tailings is below the USEPA's recommended limits. Although gaseous mercury emissions from a cinnabar stockpile increase in summer, the measured levels do not reach the WHO's recommended limit. The Enrichment Factor and  $I_{geo}$

indexes for As, Cd, Hg, Pb, Sb and Zn indicate strong to extreme contamination in the mine ponds and moderate contamination in the colluvial sediments/metasediments. Aeolian dispersion is the most important contaminant agent. The surrounding soils show strong to extreme levels of Hg and moderate to extreme levels of As, Cd, Pb and Sb. Restoration of these abandoned wastes is recommended to reduce the health risks for residents and tourists due to this aeolian contaminant dispersion.

**Keywords:** Potentially hazardous elements; Acid mine drainage; Electrical resistivity tomography; Tailings dune; San Quintín mine; Don Quixote Route

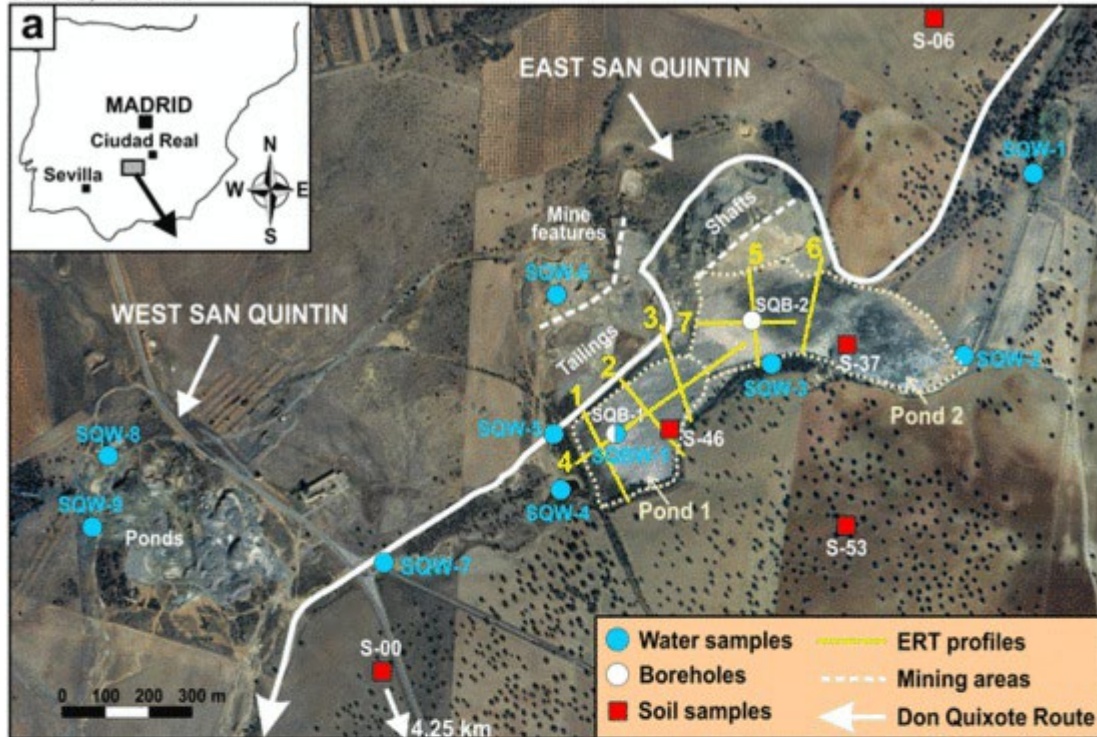
## 1 Introduction

Spain has a long mining tradition dating from pre-historic times up to the present day, although extensive mining operations have caused resource depletion in many areas. The cessation of mining activity has generated a large amount of mine wastes, typically from mines that were abandoned up until the 1980s, most of which represent geochemical hazards (Rodríguez and Gómez, 2006). Mine tailings are watery sludge composed of medium-to-fine-grained material, resulting from grinding and mineral processing (e.g., galena, pyrite, chalcopyrite, arsenopyrite). They are piled up as less than 5 cm thick sedimentary sequences and are differentiated by slight granulometric and/or compositional properties. They entail both an accumulation and a potential subsequent emission source of trace elements (Cu, Fe, Pb, Zn, etc.) with formation of Acid Mine Drainage (AMD) due to the oxidation of sulfides present in the mine tailings, either because they were not properly benefited and stored or due to the lack of an appropriate extractive technology during the time they were exploited. Mine ponds are, therefore, an important environmental problem, especially if they contain abandoned deposits.

The San Quintín abandoned mine tailings, located in the Ciudad Real province to the north of Puertollano (Spain), are crossed by the Don Quixote Route ([www.castillalamancha.es/sites/default/files/ruta\\_dqm\\_mapa\\_esp.zip](http://www.castillalamancha.es/sites/default/files/ruta_dqm_mapa_esp.zip)), a tourist set of itineraries that the government created in 1995 to celebrate the IV Centenary of the publishing of “El ingenioso hidalgo Don Quijote de La Mancha” (Fig. 1a). This route, the longest ecotourist route in Europe, has already been declared as Cultural Itinerary by the Council of Europe, and soon it could reach the rank of Humanity Heritage because

of its high environmental and cultural quality. These features therefore make the San Quintín mining group a busy tourist route, which is why its environmental characterization of potential hazards is so necessary.

387900, 4298400



390375, 4296750



Fig. 1 a) Location of the San Quintín mine site and the Don Quixote Route. Sampling points (boreholes, soil and water samples) are displayed; b) mining facilities ruins at East San Quintín; c) acid mine drainage from the tailings at East San Quintín; d) tailings dune migrating towards agricultural soils; and e) Tirteafuera river crossing the mining site.

In this work, we have applied mineralogical and geochemical characterization techniques and shallow, non-destructive geophysical techniques (Electrical Resistivity Tomography) to obtain a detailed picture of the mine ponds geometry, the composition and thickness of its infilling, the possible existence of water flows within the ponds, and the occurrence of AMD leaks. This study has been conducted to: 1) characterize the present condition of the mine tailings, 2) survey possible sites that could cause health risks for residents and tourists on the Don Quixote Route, and 3) set the basis for a hypothetical reclamation plan that raises the value of this zone as both a cultural and geological heritage site.

During the last few years, interest of the research community in relation to the characterization and management of abandoned mine deposits has been continuously increasing. This topic acquires special relevance when protected or environmentally sensitive areas are concerned, such as National Parks and zones of special interest, due to their cultural and/or geological heritage. In this sense, the application of different multidisciplinary techniques allowing us to characterize the mine deposits, and its potential as a pollution source is of crucial importance. Although different environmental works of such areas can be found in the literature, they generally focus on reduced aspects of the characterization of mine deposits. The case study described in this work constitutes a clear example of how the combination of different disciplines, such as geochemical, geological, geophysical and hydrogeological methods, can provide a more complete framework in which an integral characterization of the deposits, using mainly non-destructive methods, is achieved. The novelty of this work comes from the scarcity of examples dealing with how the integration of multiple independent techniques can be successfully implemented.

## **2 Location and features of the mine site**

The San Quintín mining group is located to the north of Puertollano (Ciudad Real, Spain). This mining group is composed of two mining zones: East and West San Quintín (Fig. 1a). The ore is mainly composed of intensively exploited Ag-bearing galena and sphalerite as essential phases of a complex hydrothermal mineralization also including pyrite, marcasite, chalcopyrite, pyrrhotine, siderite, bournonite, boulangerite and ankerite as ore minerals (Palero et al., 1992). These Post-Variscan mineralized veins are hosted in a Precambrian metasedimentary unit. The first working data are from 1559, although the intensive exploitation began in 1606. This was performed by the Sociedad Minero-Metalúrgica de Peñarroya España (SMMP) from 1887 to 1934, i.e., the date of the mining closure. In 1973, a new flotation plant was installed for re-working of approximately three million tons of mineral from the tailings (Palero et al., 1992). Taking into account all mining works, more than 550,000 t of galena, 5000 t of sphalerite and 550 t of silver were extracted (SMMP, 1981). Furthermore, several tons of cinnabar from the Almadén mine (Ciudad Real, Spain) were experimentally treated in this new flotation plant with successful results. At present, the San Quintín mining group is abandoned, and the ruins of the mine structures, together with several mine tailings resulting from re-working, are clearly recognized (Fig. 1b, c). Acid mine drainage from the tailings is visible. Furthermore, a tailings dune, formed over one of the ponds, is migrating towards the surrounding agricultural soils (Fig. 1d). The course of the Arroyo de la Mina stream, which crosses the mining area, was altered and actually runs along the edge of the mine ponds (Fig. 1e).

## **3 Methodology**

Geophysical, mineralogical and geochemical techniques have been applied to determine the geometry and composition of mine ponds and the possible occurrence of AMD. Seven electrical resistivity tomography profiles were surveyed, and re-worked tailing samples of two ponds, five soil samples, nine water samples and gaseous mercury emissions were analyzed by XRD, ESEM-EDX, TD, FUS ICP-MS and ZAAS-HFM respectively.

### **3.1 Description of sampling**

Non-disturbed rock drill core samples were collected from two boreholes using a TECOINSA TP-50/400 rotary drilling machine with a minimum core bit diameter of 86 mm. The sampling depth was of 10 m in the borehole located in the pond 1 (SQB-1) and 12 m located in the pond 2 (SQB-2) (Fig. 1a). Sampling was carried out by digging down below the surface of each pond, casting aside the parts corresponding to surficial sealing to prevent the wall material from falling inside the borehole during drilling.

Seven unaltered samples were collected at the SQB-1 borehole, and nine samples at the SQB-2 borehole. All samples were air-dried for 7 days, passed through a 2-mm sieve, homogenized, and stored in plastic bags at room temperature prior to laboratory analyses. One water sample was also collected at 8.5 m depth from SQB-2. Furthermore, five representative soils were also sampling: four of them in the studied zone and the last one from a natural soil located 4.25 km south east of the mining area as a background sample. In addition to this, Total Gaseous Mercury (TGM) was measured using a 200 m sample spacing grid on summer and winter by means of an Atomic Absorption Spectrometer with Zeeman Effect (ZAAS-HFM). Finally, nine water samples were collected in June in 250 mL plastic bottles at different points of the watercourse crossing the mining area (Fig. 1e). Water samples were kept in refrigerator at 4 °C and, prior to analysis, were filtered with 45 µm pore spacing.

### **3.2 Geophysical method**

Electrical Resistivity Tomography (ERT) is a shallow geophysical prospecting technique which involves measuring a series of resistivity profiles by selected sets of an electrode array, so that increasing separation between the electrodes provides information from increasingly greater depths. The principal applications of this technique (i.e., Telford et al., 1990; Reynolds, 1997; Šumanovac, 2006) include the definition of aquifer boundary units, the detection of voids, the mapping of saltwater intrusions into coastal aquifers, the identification of contaminated groundwater plumes, the detection of mineralized zones, and the exploration of sand and gravel resources among others. A Syscal Junior Switch 48 equipment was used and seven profiles were surveyed. To combine a good penetration depth, a reasonable vertical and horizontal resolution and a good signal-to-noise ratio, the Wenner–Schlumberger array was chosen (Sasaki, 1992). This array has

been successfully used by the authors in similar studies (Gómez- Ortiz et al., 2010a; Martín-Crespo et al., 2010a, 2011, 2012) because of the high resistivity contrast between the vase of the mine ponds and their infilling.

The resistivity field data comprise resistance measurements between various electrodes and related geometry information. An apparent resistivity value is calculated, which depends only on the resistance measurements and the array geometry. These data are plotted as a pseudosection, which is a plot of the apparent resistivity values based on the geometry of the electrodes. Pseudosections are difficult to work with and require conversion into sections with true resistivity values and depths through a data inversion procedure that facilitates interpretation. In this study, inversion of resistivity data was performed using RES2DINV code (Loke and Barker, 1996). For each data set, L1 norm was used for the data misfit and the inversion was performed using the L1 norm (robust) for the model roughness filter (Loke et al., 2003). Robust inversion is more capable of handling sharp boundaries in the model and was used in all inversions, due to the expected large contrasts in electrical properties of the involved materials. The method uses a finite element scheme for solving the 2-D forward problem and blocky inversion method for inverting the ERT data. RES2DINV generates the inverted resistivity image for each line. The quality of the inversion result was checked by monitoring absolute error (eabs) between the measured and predicted apparent resistivity given by, where and are the measured and calculated apparent resistivity values at the data point, respectively, and N is the total number of data points. The inverted section is then used to interpret the subsurface lithology. Data processing consists of removing bad data points, including the topography data along the profile.

### **3.3 Mineralogical and geochemical methods**

Mineralogical characterization of the borehole and soil samples was performed by X-ray diffraction (XRD) using a Philips X'Pert powder device with a Cu anticathode and standard conditions: speed 2° /min between 2° and 70° at 40 mA and 45 KV.

The whole sample was examined by crystalline non-oriented powder diffraction on a side-loading sample holder. Semi-quantitative results were obtained by the normalized reference intensity ratio (RIR) method. The mineralogy of the samples was also studied



by environmental scanning electron microscopy (ESEM), coupled with energy dispersive X-ray analysis (EDX), using a Philips XL30 microscope. The ESEM was operated at a low-vacuum mode, at a pressure between 0.5 and 0.6 Torr under a water vapor atmosphere and an operating voltage of 20 kV. The XRD and ESEM-EDX analyses were performed at the Centro de Apoyo Tecnológico (CAT Universidad Rey Juan Carlos, Móstoles, Spain). From the total list of major, minor and trace elements analyzed, Ag, As, Cd, Cu, Fe, Hg, Pb, S, Sb, and Zn were specially chosen for this study because of their abundance in these types of sludges and because most of them are included in the priority contaminant list of environmental protection agencies (US EPA, 1993). They were analyzed by TD (Total Digestion) or FUS (lithium metaborate/tetraborate fusion) ICP-MS (Inductively Coupled Plasma-Mass Spectrometry) at the Activation Laboratories Ltd. (1428 Sandhill Drive, Ancaster, Ontario, Canada). Quality control at the Actlabs laboratories is performed by analyzing duplicate samples and blanks to check the precision, whereas accuracy is determined using Certified Reference Materials (GXR series; see <http://www.actlabs.com>). Detection limits for the analyzed elements are as follows (data in  $\mu\text{g/g}$ ): Ag (0.3), As (5), Cd (0.5), Cu (1), Fe (100), Hg (0.005), Pb (5), S (10), Sb (0.5), and Zn (1). Pb content higher than 5000  $\mu\text{g/g}$  (above the ICP-MS maximum detection limits) was measured by ICP-OES.

Water samples were analyzed by ICP-MS at Activation Laboratories Ltd. (same reference as above). The pH was measured using an electronic pH meter (CRISON) that was calibrated at two points (at pH of 7 and 4) using standard buffer solutions. This parameter was determined in a slurry system with an air-dried sample (10 g) mixed with distilled water (25 mL). Before reading the pH values, these solutions were vigorously stirred in a mechanical shaker for 10 min and left to stand for 30 min.

#### **4 Results and discussion**

The results of the mineralogical and geochemical characterization of the samples collected from boreholes, soils and water, and those obtained from the geophysical study concerning the structure and infilling of ponds and the possible presence of acid water flows are presented here.

## 4.1 Mine pond structure

The geometry of both mine ponds was determined from the ERT survey, and the results have been interpreted with the help of the borehole analysis data.

### 4.1.1 Mine pond 1

From the exploratory borehole SQB-1, a thickness of 8.3 m of infilling pond material was observed before the top of the Quaternary colluvial deposits was reached. The recovered material includes detrital sediments characterized by dry, unconsolidated coarse sands, corresponding to the re-worked tailings. Between 8.3 and 10 m depth of quaternary colluvial deposits were found, composed of gravel (mainly quartzite) and sandy detrital materials (8.3 to 9 m depth) and gravely (highly weathered metasediments) sediments (9 to 10 m depth). After reaching the quaternary deposits, the drilling stopped at 10 m depth. The water table was reached at 8 m, just 0.3 m above the colluvial deposits. Consequently, most of the mine pond infilling was found under dry conditions.

Four ERT profiles were measured (Fig. 1a). Profiles 1–3 (235 m long each) are transverse to the mine pond, whereas profile 4 (475 m long) is longitudinal to it. Three main resistivity units can be distinguished (Fig. 2): an upper unit with low to high ( $\sim 5$  to  $600 \Omega\cdot\text{m}^{-1}$ ) resistivity values, corresponding to the mine pond infilling; a medium resistivity ( $20\text{--}50 \Omega\cdot\text{m}^{-1}$ ) intermediate unit associated with the quaternary colluvial deposits, and a high resistivity ( $> 200 \Omega\cdot\text{m}^{-1}$ ) lower unit corresponding to the Precambrian metasediments. The upper unit displays high resistivity values associated with the upper dry sandy materials observed in the borehole, but lower resistivity values at depth, especially at the SW end of the mine pond (profile 1, NW end of profile 2 and SW end of profile 4). A visual inspection of these zones in the field revealed the presence of vegetation indicating water infiltration, indicating these low resistivity areas as the same sandy materials but under wet conditions. The average infilling thickness is  $\sim 8\text{--}9$  m. The superficial discrete areas with the highest resistivity values ( $> 200 \Omega\cdot\text{m}^{-1}$ ) correspond to the location of the pond dykes. The intermediate unit is correlated with the quaternary colluvial deposits, and the four profiles reveal a north-eastward increase (from  $\sim 2$  to 10 m) in thickness. The lower unit corresponds to the top of the Precambrian metasediments that deepen towards the NE in a staircase-like geometry, which is

consistent with the thickness increase of the quaternary deposits. The easternmost end of profile 4 displays a low resistivity unit that represents the infilling of mine pond 2, extending to the east, and partially covered by a medium resistivity superficial area of ~ 80 m in length (355 to 435 m of profile 4), which corresponds to the aeolian deposits coming from the upper part of mine pond 1.

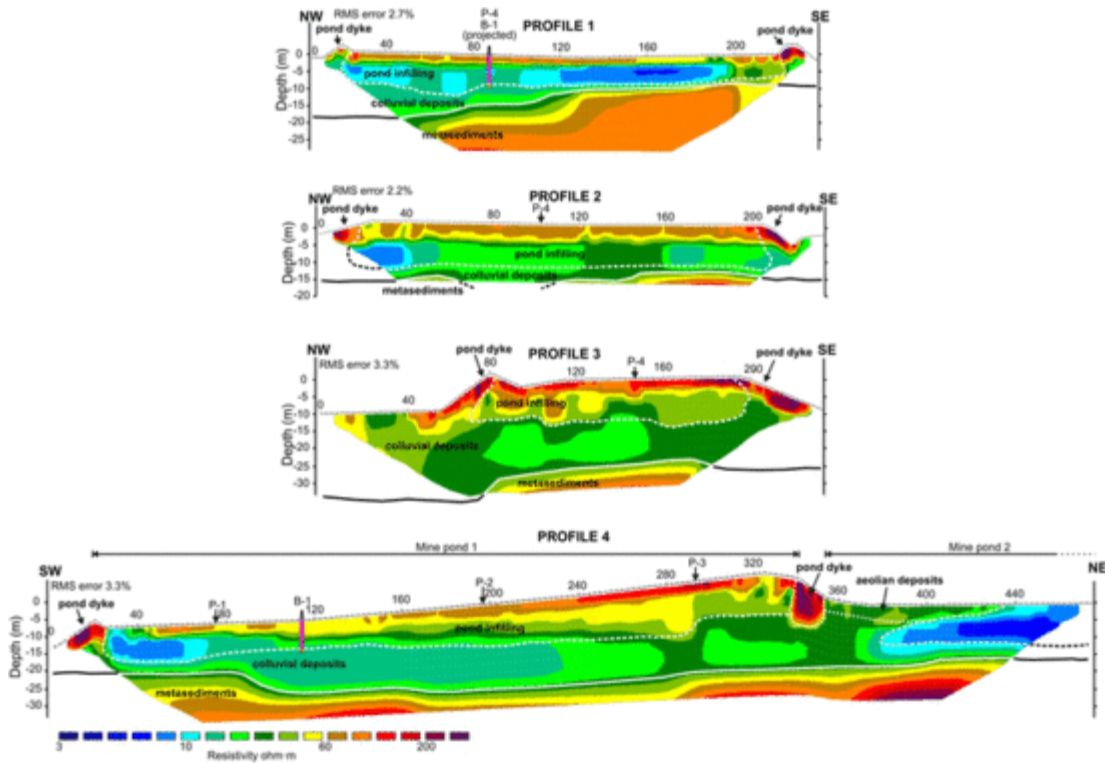


Fig. 2 ERT profiles carried out at mine pond 1. The location of the borehole SQB-1 and its corresponding lithological units used to interpret the different resistivity layers is also shown. The thickness of the infilling materials, as well as the geometry of the base of the mine pond and the thickness of the colluvial deposits is imaged. See text for detailed explanation.

#### 4.1.2 Mine pond 2

The second exploratory borehole SQB-2 provided 8 m of mine tailings 3.30 m of alternating gravel, sands and clays corresponding to the quaternary colluvial deposits and 0.70 m of Precambrian metasediments. Unlike the infilling pond material recovered at SQB-1, all of the samples from the first 8 m depth correspond to wet clay-rich material with very dark brown color. As in the previous case, the recovered material corresponds to the re-working of the tailings. The Quaternary colluvial material shows interbedding

of gravel (mainly quartzite), sand and clay in decimetric beds. The water table was reached at 8 m depth at the boundary between the pond infilling and the quaternary deposits. In this case, the entire mine pond infilling was found under wet conditions. Three ERT profiles were measured (Fig. 1a, 235 m long each). Profiles 5–6 are transverse to the mine pond and profile 7 is longitudinal to it. As for mine pond 1, three main resistivity units can be distinguished (Fig. 3) however, the intermediate and lower units have similar characteristics. The upper unit is defined by low resistivity values ( $\sim 3$  to  $20 \Omega\cdot\text{m}^{-1}$ ). This lower resistivity is explained by the fine-grained materials that characterize the infilling of mine pond 2, as well as their high water content. Similar to mine pond 1, the average infilling thickness of this mine pond is  $\sim 8$  m. Only small areas of moderate to high resistivity values ( $> 60 \Omega\cdot\text{m}^{-1}$ ) are displayed at the surface corresponding to the presence of pond dykes. Similar to mine pond 1, the intermediate and lower units are correlated with Quaternary colluvial deposits and Precambrian metasediments, respectively. Beneath mine pond 2, the thickness of the Quaternary deposits ranges from  $\sim 3$  to  $10$  m, whereas the top of the Precambrian metasediments can be found at a relatively constant depth of  $\sim 12$  m below the ground surface.

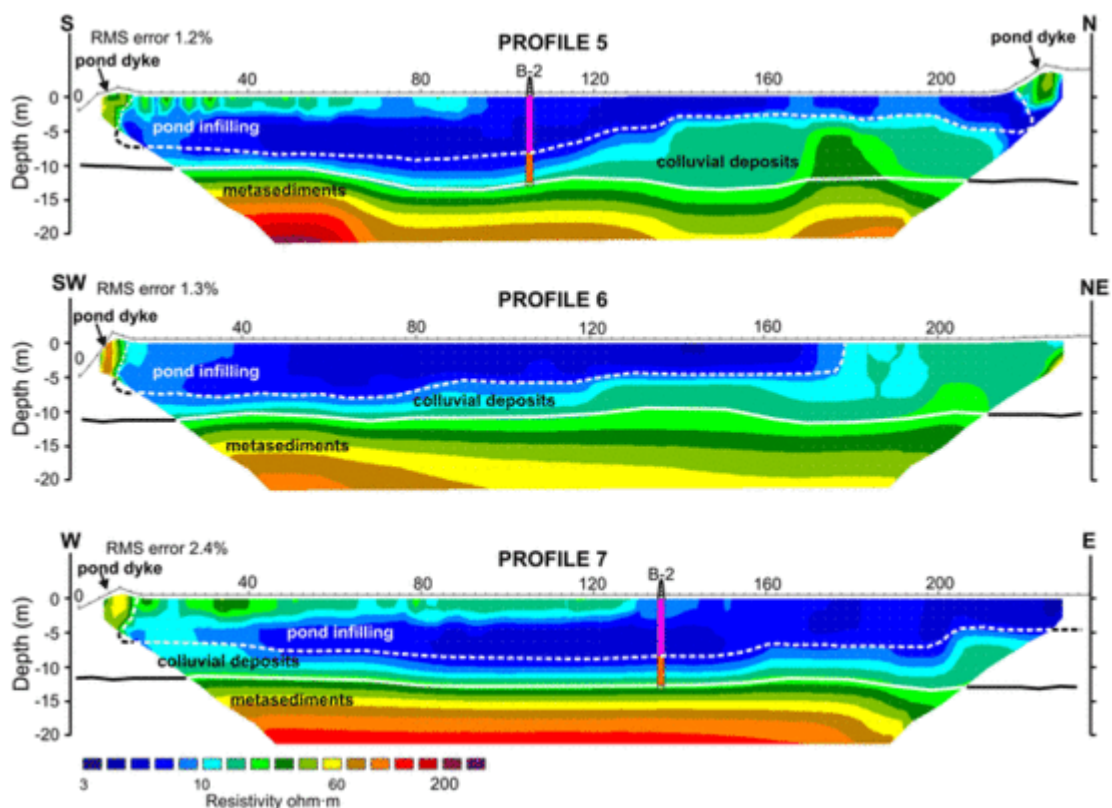


Fig. 3 ERT profiles carried out at mine pond 2. The boundaries of the different lithological units were defined using the information provided by the borehole SQB-2. Same information for the Fig. 2. See text for detailed explanation about the interpreted units.

#### 4.2 Mineralogical characterization of ponds

A nearly homogeneous mineralogical composition can be inferred from the X-ray diffraction data (Table 1). The mine tailings are mainly composed of quartz (60–90%), illite (5–25%) and chlorite (5–10%), with gypsum, cinnabar and sphalerite as minor phases. The lower illite content corresponds to colluvial sediment of mine pond 2, collected between 8.30 and 10 m depth. The highest clay mineral content was identified at the bottom of the ponds, corresponding to Precambrian metasediments (highly weathered in the SQB-1 borehole). Significant amounts of secondary gypsum and minor amounts of feldspar in the first few meters were identified in both ponds. Primary ore minerals were not identified by X-ray Diffraction due to the optimized mining works (except for sphalerite in sample 3 from the SQB-2 borehole). Pyrite, galena, chalcopyrite and gangue minerals (barite) were identified by ESEM-EDX. The transition to the in situ host rock was sharp. Cinnabar was identified in sample 3 from the SQB-1 borehole. Its presence is related to the experimental metallurgical works conducted during the last period of operations in the Almadén mine, the world's largest mercury mining district, which was also operated by SMMP.

Table 1 Semi-quantitative mineralogical composition (wt.%) of the studied samples from the San Quintín boreholes (SQB). Qtz: quartz, Ill: illite; Chl: chlorite; Fsp: feldspar; Gp: gypsum; Ci: cinnabar; Sp: sphalerite.

Borehole		Sample	Depth (m)	Qtz	Ill	Chl	Fsp	Gp	Ci	Sp
SQB-1	Pond	1	0.50	75	5=10	5	1=5	5		
		2	3.00	75	10	10		5		
		3	5.30	80	10	5=10		1=5	1=5	
		4	8.10	80	15		1=5	1=5		
	Colluvial	5	8.70	90	5=10	1=5				
		6	9.00	70	20	10				
		7	10.00	65	25	10				
SQB-2	Pond	1	0.50	60	20	15	1=5	1=5		
		2	3.00	70	15	10	1=5	1=5		
		3	6.00	70	20	10		1=5		1=5
	Colluvial	4	8.00	90	1=5	1=5				
		5	8.20	90	5		1=5			
		6	9.00	85	10	1=5				
		7	10.00	90	1=5	1=5				
	Meta	8	11.50	60	30	10				
		9	12.00	60	25	5=10				

### **4.3 Geochemical constraints**

#### **4.3.1 Mine tailings and soils**

The compositions of boreholes SQB-1 and SQB-2 are similar, characterized by significantly high As, Cd, Hg, Pb, Sb and Zn content, and low Ag content (Table 2). The highest contents are displayed in the pond samples, the intermediate contents are observed in the colluvial material samples, and the lowest contents are seen in the metasediment samples. The ponds were not waterproofed, and the underlying colluvial sediments were contaminated by hazardous metals from the upper ponds. The As content ranged between 8 and 54  $\mu\text{g/g}$ , Pb ranged from 33 to 10,500  $\mu\text{g/g}$  and Zn ranged from 165 to 4470  $\mu\text{g/g}$ . Other trace elements that displayed high values included Cd (up to 22.4  $\mu\text{g/g}$ ), Cu (up to 381  $\mu\text{g/g}$ ), and Sb (up to 74  $\mu\text{g/g}$ ). The high Hg content (up to 125  $\mu\text{g/g}$ ) is related to the experimental metallurgical works previously cited, and similar values have been reported in soils from the Almadén district (Higuera et al., 2006; Millán et al., 2006). Because of the re-working of approximately three million tons of minerals from the tailings, the highest contents are located at the upper levels of both ponds: 0 to 8 m at borehole 1, and 0 to 6 m at borehole 2. Montoya-Montes et al. (2012) explained the mining company increased the ponds size from 1977 to 1984 to provide space for these re-worked tailings. In a preliminary study, Gómez-Ortiz et al. (2010a) reported similar or slightly higher metal contents than the equivalent samples of the present study. Rodríguez et al. (2009) reported similar high Cd, Cu, Pb and Zn contents. Both works were only used surficial pond samples. In the present study, the whole thickness of the tailing pond deposits have been drilled and analyzed, providing a detailed picture of the remaining, potentially hazardous element contents.

Table 2 Fe<sub>2</sub>O<sub>3</sub> total and trace elements content in the San Quintín samples: borehole (SQB), background (S-00), agricultural (S-06 and S-53) and mine soils (S-37 and S-46).

Sample		Depth	Ag	As	Cd	Cu	Fe <sub>2</sub> O <sub>3</sub> <sub>TOT</sub>	Hg	Pb	S	Sb	Zn
		(m)	(µg/g)	(µg/g)	(µg/g)	(µg/g)	(wt.%)	(µg/g)	(µg/g)	(wt.%)	(µg/g)	(µg/g)
SQB 1.1	Pond	0.50	6	19	5.1	42	4.45	47.8	1560	0.28	37.2	1250
SQB 1.2		3.00	4.6	18	18	50	4.78	2.1	1560	0.32	36	3210
SQB 1.3		5.30	6.5	16	13.1	64	5.22	125	2000	0.30	45.3	2400
SQB 1.4		8.10	6.7	23	5.8	236	6.15	2.6	1510	0.29	44.2	1250
SQB 1.5	Colluvial	8.70	2.9	24	1.8	196	7.43	0.42	417	0.10	26.9	537
SQB 1.6		9.00	2	13	2.6	71	6.62	1.6	462	0.11	15.3	539
SQB 1.7		10.00	0.4	8	0.6	38	6.75	0.2	79	0.02	5	186
SQB 2.1	Pond	0.50	10.9	20	12.9	75	6.26	3.6	4440	0.36	74.3	2280
SQB 2.2		3.00	29.1	48	11.1	353	6.05	2.1	10,500	0.59	155	2070
SQB 2.3		6.00	22.4	54	22.4	381	6.34	67.3	6380	0.95	162	4470
SQB 2.4	Colluvial	8.00	2	20	6.8	53	5.37	1.4	483	0.15	24.6	844
SQB 2.5		8.20	2.4	21	7.1	74	5.27	0.4	577	0.13	26.4	837
SQB 2.6		9.00	0.8	21	0.8	52	9.46	0.3	102	0.03	39.8	313
SQB 2.7		10.00	0.6	14	1	52	7.39	0.5	83	0.05	26.9	267
SQB 2.8	Meta	11.50	0.3	12	0.5	36	6.54	0.04	33	0.02	27.8	165
SQB 2.9		12.00	0.5	12	0.6	68	6.17	0.2	49	0.03	16.2	253
S-00	Soil	0.15	0.2	11	b.d.	18	4.15	0.12	34	0.01	1.9	49
S-06		0.15	0.3	b.d.	b.d.	5	1.67	1.12	41	0.01	2.1	34
S-53		0.15	0.3	12	b.d.	10	4.67	1.45	66	0.01	1.9	55
S-37		0.15	0.4	6	b.d.	12	3.57	163	56	0.09	2.2	71
S-46		0.15	3.1	26	6.8	39	4.12	185	1110	0.28	29.8	1180

Five representative soil samples from the area were analyzed to determine the significance of contamination (Table 2; Fig. 1). The mine soil samples (S-37 and especially S-46) show similar metal and As content to the upper borehole samples. The agricultural soil samples (S-06 and S-53) show significantly lower metal and As content, but higher Hg and Pb contents than the background sample S-00 from an agricultural soil 4.5 km to the south-east. However, remarkable high As, Pb and Zn contents were still found in this S-00 background sample, suggesting that the contamination of surrounding agricultural soils is significant.

Statistical data processing was performed using Minitab 15 software. The multivariate analysis was based on clustering (simple linkage dendrograms) of the set of samples and significant metals (Ag, As, Cd, Cu, Hg, Pb, Sb, and Zn). The dendrogram (cluster analysis) of the metals and As in the samples from the tailings (Fig. 4a) reflects the metallic signature of the district (Pb—Ag—Sb, Cu and Zn—Cd to a certain extent, Palero et al., 1992), with As mainly related to Sb (bournonite, boulangerite) and Pb—Ag (galena) (Table 2). Some samples display Cd—Zn affinity, whereas other samples display greater affinity to the Ag—Pb—Sb—As association. The highest distances obtained for Hg reflect its external origin. The cluster analysis also shows the extremely low distance of the samples from both boreholes (Fig. 4b) due to their common origin. In general, the samples are grouped by their origin independently of the borehole, consistent with the higher metal contents of the pond and colluvial samples, and the lower contents of the metasediments. Only the SQB 2.2 sample showed a slightly higher distance, probably due to slightly higher Ag and Pb contents.

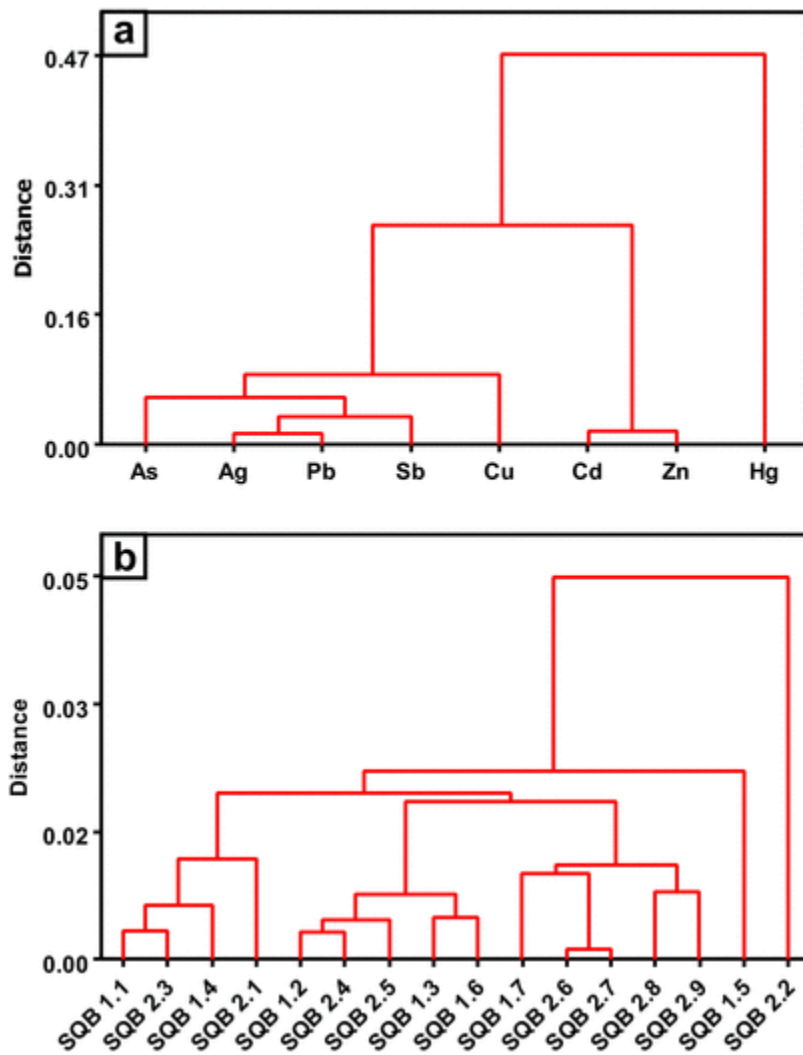


Fig. 4 a) Dendrogram (distance: simple) of metals from both borehole samples; b) dendrogram (distance: simple) of all samples, showing significantly low distances.

#### 4.3.2 Water samples

Table 3 comprises the results of the borehole, water and AMD water analyses (sample locations in Fig. 1a). The SQBW-1 sample was collected at 8 m depth in borehole SQB-2. The high Electrical Conductivity (EC) and slightly acidic pH values are consistent with water retained in tailing ponds from ore deposits such as San Quintín. Samples SQW-5 and SQW-6 (East San Quintín) indicate AMD flowing from the remaining tailings: low pH, high conductivity and significantly high trace element concentrations (Cd, Cu, Ni > 2000 µg/L; Zn > 130,000 µg/L; Pb > 370 µg/L; and Fe > 99,000 µg/L). Sample SQW-9 from West San Quintín shows a similar pattern with significantly lower metal concentrations. This could be due to the lower volume of tailings stored in this pond compared to East San



Quintín. AMD was not clearly detected in water samples from the river crossing the mine area (Fig. 1e; Table 3). pH values in these waters are neutral, and EC values and metal contents are significantly lower than in samples from the tailings. Samples SQW-1 and SQW-8, collected up- and downstream, respectively, show the lowest trace element contents. The rest of watercourse samples (SQW-2, SQW-3 and SQW-4) show higher metal contents than SQW-1 and SQW-8, indicating that trace element contamination occurs through the mining area.

Table 3. Physicochemical parameters and geochemistry of water samples: borehole 1 (SQBW), and watercourse crossing the mine site (SQW).

Sample	Type	pH	EC µS/cm	Cd µg/L	Cu µg/L	Fe µg/L	Ni µg/L	Pb µg/L	Sb µg/L	Zn µg/L
SQBW-1	Borehole	5.75	5147	3.82	12.3	90	80.1	8.49	6.07	93.6
SQW-1	Watercourse	6.19	225	0.13	1.2	90	1.8	0.59	0.12	56.9
SQW-2	Watercourse	6.94	1347	0.28	1	84	12	0.41	0.46	680
SQW-3	Watercourse	6.22	447	8.16	5.8	30	11.3	0.72	0.31	1390
SQW-4	Watercourse	7.02	4274	2.65	2	82	12.4	0.18	0.19	583
SQW-5	AMD	2.54	4413	3210	7410	99,400	3510	1690	1.3	554,000
SQW-6	AMD	2.64	3732	3020	8340	189,000	3330	377	0.29	525,000
SQW-7	Watercourse	7.15	2004	26.6	12.6	100	22.3	21.6	0.67	2520
SQW-8	Watercourse	6.51	971	3.42	4.9	60	2.9	16.6	2.96	510
SQW-9	AMD	4.28	1547	1020	1290	140	296	2820	1.27	138,000

b.d. below detection.

#### 4.3.3 Total Gaseous Mercury (TGM)

Gaseous mercury emissions from the tailings and surrounding soils were measured due to the significantly high Hg content in the mine ponds. The geostatistical treatment of data was performed applying block kriging (Cressie, 1990) to obtain interpolation maps of the study area. Previously, a semivariogram of experimental mercury vapor data were obtained using variance and fitted to a spherical model (Pannatier, 1996). The TGM distribution in the studied area differs widely between summer and winter (Fig. 5a and b respectively and Table 4), especially in areas affected by mercury (values as high as the United States Environmental Protection Agency (USEPA) standards) for chronic exposure (200 ng m<sup>-3</sup>) (US EPA, 2007). In winter the area affected by TGM values up to 100 ng m<sup>-3</sup> is restricted to the surroundings of the cinnabar stockpile, but in summer, the affected area is 0.16 km<sup>2</sup>, and extends into the Don Quixote Route. This area reaches TGM values lower than the World Health Organization (WHO) recommended limit for the general population (1000 ng m<sup>-3</sup>) in the worst scenario (WHO, 2000), with higher temperature and solar radiation during summer. In terms of risk assessment, the gaseous mercury emissions in this area do not pose a risk for the general population.

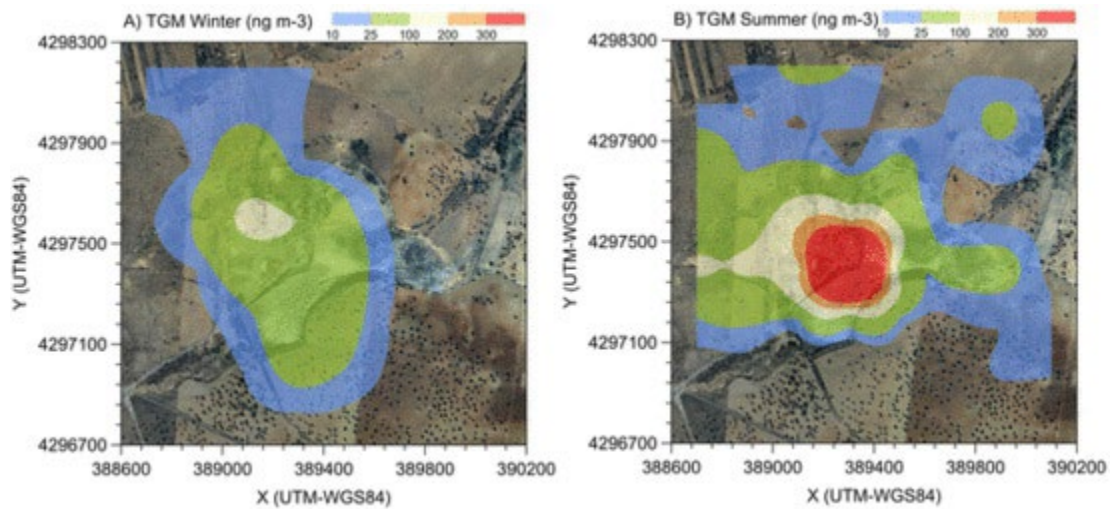


Fig. 5 Total Gaseous Mercury (TGM) seasonal distribution on the study area: a) winter, and b) summer values.

Table 4 Statistical summary of Total Gaseous Mercury (TGM) in the study area.

	TGM (ng·m <sup>-3</sup> )	
	Winter	Summer
Number of samples	64	64
Minimum value	2	2
Maximum value	139	1219
Average value	15	44
Geometric mean	7	13

#### 4.4 Environmental concerns

Potential environmental concerns can be divided into three broad categories: (i) ecosystem risks, (ii) human health risks and (iii) physical hazards. Ecosystem risks (associated with acidity and a range of metals) and physical hazards (open shafts, unstable ponds) are broadly found in the San Quintín mine group (Fig. 1b–d). Human health risks could be associated with the aeolian dispersion of contaminants.

Concentrations of trace elements in AMD water samples are very high, reaching levels beyond the USEPA's maximum recommended limits of these elements in irrigation waters (Cd 10 µg/L; Cu 200 µg/L; Fe 5000 µg/L; Ni 200 µg/L; Pb 5000 µg/L; Zn 2000 µg/L; US EPA, 2012). This is the case for Cd, Cu, Fe (except for SQW-9), Ni and Zn, whereas Pb limits are not exceeded. Water and borehole sample metal contents are lower than these recommended limits, denoting that the river crossing the mining area is not significantly affected by AMD. Clay minerals, which are present in significant amounts in the pond tailings (illite + chlorite, Table 1) could act as hosts for metal sorption, thus preventing significant percolation of heavy metals to the river.

Ecosystem and human risks were assessed using the Enrichment Factor (EF) and the Geoaccumulation Index ( $I_{geo}$ ). EF was used to assess the level of contamination and the possible anthropogenic impact (Sutherland, 2000). To identify anomalous metal concentration, geochemical normalization of the heavy metals data to a conservative element, such as Fe, was employed (geochemical normalization). EF was calculated using the formula  $EF = (M/Fe)_{sample} / (M/Fe)_{background}$ , where  $(M/Fe)_{sample}$  is the ratio of metal to Fe concentrations in the sample and  $(M/Fe)_{background}$  is the ratio of metal to Fe concentrations of the background (sample S-00; Table 2). Sutherland (2000) proposed five contamination categories: minimal enrichment ( $EF < 2$ ), moderate enrichment ( $2 < EF < 5$ ), significant enrichment ( $5 < EF < 20$ ), very high enrichment ( $20 < EF < 40$ ) and extremely high enrichment ( $EF > 40$ ). EF values are quite similar in both boreholes samples (Table 5). The borehole samples show very high to extremely high enrichment in Ag, Cd, Hg, Pb, Sb, and Zn. Deeper samples display a progressive decrease. EF values for As are significantly lower than for the rest of elements, reflecting the lack of As-bearing minerals. Agricultural soil samples (S-06; S-53) and mine soil sample (S-37) show minimal or moderate enrichment for Ag, As, Cd, Cu, Pb, Sb and Zn. The mine soil sample S-46 shows significantly higher enrichment in all of these elements. This is due to the re-working of tailings from 1973 to 1988, which were mainly accumulated in this pond (Montoya-Montes et al., 2012). The EF values for Hg were significant or very high for agricultural soils and extremely high for mine soils. These data highlight the significant metal contents of the mine site, which can become especially hazardous due to aeolian dispersion. In fact, Hg content of all water samples analyzed was  $< 0.2 \mu\text{g/L}$ , denoting the aeolian character of the contamination.

Table 5 Enrichment factor (EF) of San Quintín samples: borehole (SQB), agricultural soils (S-06, S-53) and mine soils (S-37, S-46).

Sample		Depth (m)	Ag	As	Cd	Cu	Hg	Pb	Sb	Zn
SQB 1.1	Pond	0.50	27.98	1.61	23.78	2.18	371.48	42.79	18.26	23.79
SQB 1.2		3.00	19.97	1.42	78.14	2.41	15.19	39.84	16.45	56.88
SQB 1.3		5.30	25.84	1.16	52.07	2.83	828.14	46.77	18.95	38.94
SQB 1.4		8.10	22.61	1.41	19.57	8.85	14.62	29.97	15.70	17.21
SQB 1.5	Colluvial	8.70	8.10	1.22	5.03	6.08	1.95	6.85	7.91	6.12
SQB 1.6		9.00	6.27	0.74	8.15	2.47	8.36	8.52	5.05	6.90
SQB 1.7		10.00	1.23	0.45	1.84	1.30	1.02	1.43	1.62	2.33
SQB 2.1	Pond	0.50	36.13	1.21	42.76	2.76	19.89	86.57	25.92	30.85
SQB 2.2		3.00	99.81	2.99	38.07	13.45	12.00	211.84	55.96	28.98
SQB 2.3	Colluvial	6.00	73.31	3.21	73.31	13.86	367.11	122.83	55.81	59.71
SQB 2.4		8.00	7.73	1.41	26.28	2.28	9.02	10.98	10.01	13.31
SQB 2.5		8.20	9.45	1.50	27.96	3.24	2.62	13.36	10.94	13.45
SQB 2.6		9.00	1.75	0.84	1.75	1.27	1.10	1.10	9.19	2.80
SQB 2.7		10.00	1.68	0.71	2.81	1.62	2.34	1.37	7.95	3.06
SQB 2.8	Meta	11.50	0.95	0.69	1.59	0.51	0.21	0.62	9.28	2.14
SQB 2.9		12.00	1.68	0.73	2.02	2.54	1.12	0.97	5.73	3.47
S-06	Soil	0.15	3.73	0.90	3.73	0.69	23.19	3.00	2.75	1.72
S-53		0.15	1.33	0.97	1.33	0.49	10.74	1.73	0.89	1.00
S-37		0.15	2.32	0.63	2.91	0.77	1579.01	1.91	1.35	1.68
S-46		0.15	15.61	2.38	34.25	2.18	1552.89	32.88	15.80	24.26

$I_{geo}$  was defined by Müller (1969) and enables the assessment of contamination of sediments by comparing current and pre-industrial concentrations of heavy metals. This index is mathematically expressed as  $I_{geo} = \log_2 C_n/1.5B_n$ , where  $C_n$  is the concentration of an element in the sediment sample and  $B_n$  is the background concentration of that element in Earth's crust, according to Taylor and McLennan (1995). The factor 1.5 is used to address possible variations due to lithogenic effects. Müller (1969)

suggested 6 descriptive classes: uncontaminated ( $I_{geo} \leq 0$ ), uncontaminated to moderately contaminated ( $0 < I_{geo} < 1$ ), moderately contaminated ( $1 < I_{geo} < 2$ ), moderately to strongly contaminated ( $2 < I_{geo} < 3$ ), strongly contaminated ( $3 < I_{geo} < 4$ ), strongly to

extremely contaminated ( $4 < I_{geo} < 5$ ), and extremely contaminated ( $I_{geo} > 5$ ). Metal and As  $I_{geo}$  in tailings from both ponds and soil samples were calculated and are displayed in Fig. 6. Cd, Hg, Pb and Sb show extreme contamination ( $I_{geo} > 5$ ), and As and Zn show moderate to heavy contamination ( $1 < I_{geo} < 5$ ). The deepest samples decrease in one or two contamination classes. Cu shows moderate to heavy contamination, and Ag is classified as un-polluted. The same behavior is shown in both tailing ponds in SQB 1 and SQB 2. Samples from mine soils (S-37 and S-46) display a similar pattern to the tailings samples (Fig. 6c). Agricultural soil samples (S-06 and S-53) and the background sample (S-00) show the same features: they are moderately contaminated by As, Cd, Pb and Sb and not contaminated by Ag, Cu and Zn. The  $I_{geo}$  for Hg was strong for agricultural soils and extreme for mine soils.

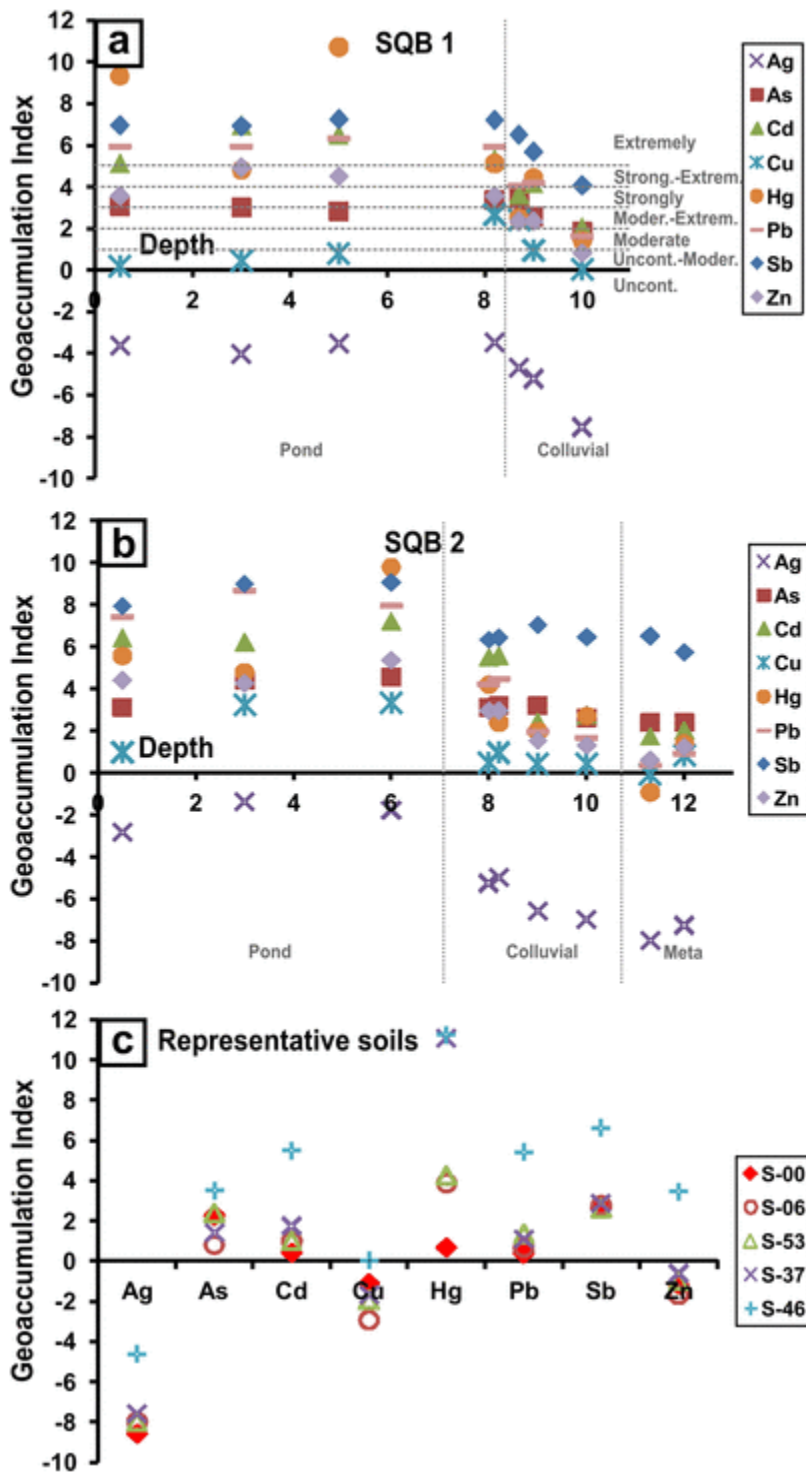


Fig. 6 Geoaccumulation Index for: a) SQB 1 borehole samples; b) SQB 2 borehole samples; c) representative soils (S-00 to S-53).

A conceptual site model is included in Fig. 7. Although several contaminant sources and pathways have been identified, aeolian dispersion of tailings seems to be the most important environmental hazard at the San Quintín mine district. Montoya-Montes et

al. (2012) and Sánchez-García et al. (2012) noted the importance of aeolian dispersion of contaminants in this mining group. Previously described in Section 2, a dune formed by the tailings dumped at the western pond of East San Quintín (Fig. 8a).

From 1984 to present, the dune has been growing and migrating towards the SW—SSW (towards the river and agricultural soils), following the dominant wind directions in the area. The latter (NNE, NE and E) coupled with moderate wind velocity ( $> 6$  m/s) maximizes the aeolian factor (Sánchez-García et al., 2012). The material balance shows that the dune loses more material than it accumulates because the tailing particles moved by the wind are not replaced. A future decrease in size or even disappearance of the dune is to be expected, as the tailings become part of the agricultural soils (Montoya-Montes et al., 2012). All obtained data indicate significant contamination issues of the agricultural soils located SW of the mining area. Ag, Cd, Pb and Zn geochemical baselines reported by Jiménez Ballesta et al. (2010) are lower than the agricultural soil samples measured in this work. Therefore, the agricultural soils surrounding San Quintín mine could be considered as contaminated. Similar research has been conducted for deposits from other Iberian Peninsula mining districts: the Iberian Pyrite Belt (Gómez-Ortiz et al., 2010b; Martín-Crespo et al., 2010a, 2011), Mazarrón (Martín-Crespo et al., 2012), Cartagena-La Unión (Martínez-Pagán et al., 2009) and Panasqueira (Grangeia et al., 2011). In all of these deposits, including the present study, the joint application of geophysical and geochemical techniques has allowed a complete characterization of sites affected by mining activities.

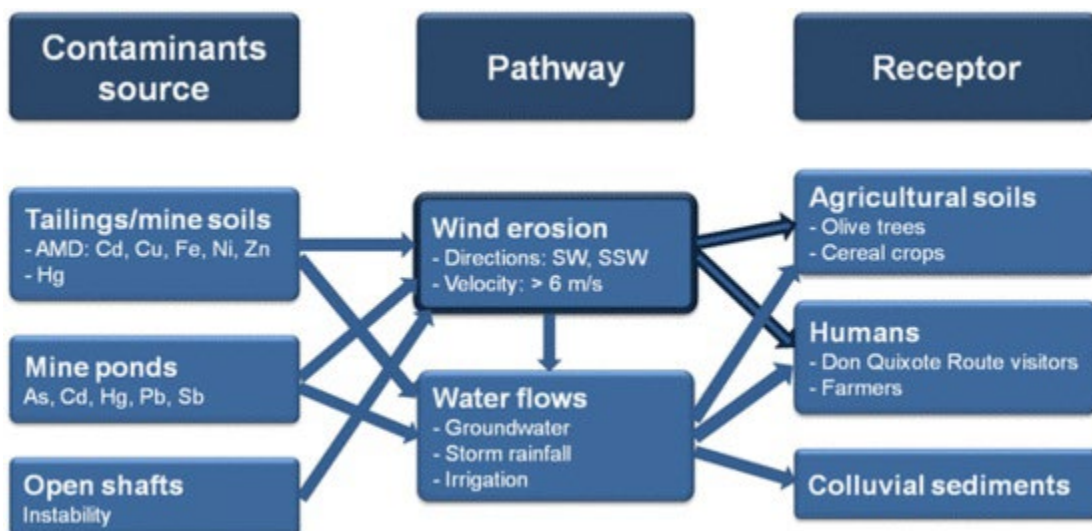


Fig. 7 Conceptual model of the sources, pathways and receptors for the San Quintín mine site.



Fig. 8 a) Tailings dune migrating towards the agricultural soils; b) schematical map of the itinerary 4 of the Don Quixote Route (Junta de Comunidades de Castilla-La Mancha, 2005); c) milestone from the Don Quixote Route at the San Quintín mine site; d) the Don Quixote Route at the San Quintín mine ponds.

The San Quintín mining group is a set of mines in the Alcudia valley and has constituted a source of wealth for the region along with the coal mining of Puertollano. Both have shaped an important part of the landscape as well as the social and economic history of the region. Although this zone is not restored, and therefore not in condition for public transit, since 2005 the San Quintín mine has been listed as one of the spots to

be visited on the so-called “Don Quixote Route, a place for adventure”, the longest Ecotourist Itinerary in Europe (Cañizares Ruiz, 2008). Its recognition, in 2007, as a European Cultural Itinerary represents its consolidation as an important cultural tourist route in an international context because it is the first itinerary created from a literary figure.

Section four of the route, called “Del Valle de Alcudia al Campo de Calatrava. Volcán, mina y dehesa”, crosses the San Quintín mining area from east to west (Fig. 8b), exhibiting tumbled down mine structures (shafts, a metallurgical plant and railways; Fig. 8c, d).

The mine railway slopes were re-used to build the pond dyke where the re-worked tailings (and the cinnabar from Almadén) were dumped. Finally, the Route continues along the second pond before carrying on towards the NW of the mine site. Furthermore, this section four of the “Don Quixote Route” continues by a drover's thoroughfare, reinforcing its attractiveness for ecotourism. The San Quintín mine has become a superb example of the cultural and socio-economic benefits that its adaptation and restoration could lend to this zone (Martín-Crespo et al., 2010b). There are several old and abandoned mines in Castilla-La Mancha that are found along the route (e.g., Minas de Horcajo; Palero et al., 2003). Although these types of tourist initiatives are noteworthy in terms of geological heritage, it is surprising that a previous characterization and reclamation work has not previously been conducted for the implementation of this new use.

The incorporation and valorization of the mining heritage, particularly inside the cultural itineraries, generates important synergies that must be taken as significant educational, environmental, socioeconomic and eco-touristic resources. However, geoenvironmental characterization, restoration and adaptation of these abandoned mines are necessary for achieving safe and pleasant transit of tourists. In the case of San Quintín, only the first step has been carried out. An excellent example of Spanish mining heritage linked to cultural itineraries is Las Médulas, a historical site in the region of El Bierzo (province of León, Spain), and the most important gold mine in the Roman Empire (Pérez-García et al., 2000). Las Médulas Cultural Landscape is listed by UNESCO as one of the World Heritage Sites. This landscape is part of the “Route of Santiago de Compostela”, proclaimed as the first European Cultural itinerary by the Council of



Europe in 1987. The route has been monitored by the Las Médulas Foundation and serves as an example of the good relationship between research, management and society at a heritage site (Orejas and Sánchez-Palencia, 2006). As a first step, an application for declaring the area as a “Heritage site of Cultural Interest” would be necessary. This protection category should reinforce the touristic valorization of mine zones such as San Quintín.

## **5 Conclusions**

This work revealed that the joint use of geophysical, mineralogical and geochemical techniques can provide an environmental characterization of abandoned mine sites, allowing for estimations of potential pollution and the extent of affected zones. An ERT survey conducted at two mine ponds revealed an ~ 8 m thickness pond infilling with different characteristics. The infilling of mine pond 1 consists of a two-unit sequence: i) an upper unit (0–5 m) corresponding to very dry loose sandy materials; and ii) a lower unit (5–8 m) corresponding to similar materials but with a higher degree of humidity. Quaternary colluvial materials occur below the infilling pond with a thickness ranging from 2 to 10 m. At mine pond 2, a homogeneous ~ 8 m thick infilling sequence is found, corresponding to wet clay-rich material. The underlying Quaternary colluvial deposits have a thickness ranging from 3 to 10 m and overlie Precambrian metasediments.

The present study reveals significant contamination from the mine tailings: at a depth of the Quaternary colluvial deposits, and at the surface of the surrounding agricultural soils. The geochemical composition of borehole samples shows significantly high contents of As, Cd, Hg, Pb, Sb and Zn. The high Hg content are related to the metallurgical works at the Almadén mine. The agricultural soil samples show lower metal and As content but higher Hg and Pb content than in the background sample. Total Gaseous Mercury emissions produce levels in the atmosphere lower than the WHO recommended limit for the general population and thus do not pose a risk for tourists of the Don Quixote Route. AMD has been identified flowing only from the remaining tailings. Ecosystem risks (associated with acidity and a range of metals) and physical hazards (open shafts, unstable ponds) are broadly found. Human health risks are associated with the aeolian dispersion of contaminants towards the surrounding agricultural soils. Considering that the San Quintín mine site is one of the spots to be

visited along the longest Eco-tourist Itinerary in Europe, it represents a major environmental hazard that needs to be characterized, monitored and restored.

#### Acknowledgements

This work has been accomplished on the frame of project URJC-CM-2008-CET-3644 funded by Comunidad de Madrid and Universidad Rey Juan Carlos. We also would like to thank Senior Editor Carranza-Torres, and three anonymous reviewers for their valuable and constructive comments to improve the quality of the manuscript.

#### References

Cañizares Ruiz M.C., La "Ruta de Don Quijote" en Castilla-La Mancha (España): nuevo itinerario cultural europeo, *Nimbus* 21–22, 2008, 55–75.

Cressie N.A.C., The origins of kriging, *Math. Geol.* 22, 1990, 239–252.

Gómez-Ortiz D., Martín-Crespo T. and Esbrí J.M., Geoenvironmental characterization of the San Quintín mine tailings, Ciudad Real (Spain), *Dyna* 161, 2010a, 131–140.

Gómez-Ortiz D., Martín-Velázquez S., Martín-Crespo T., De Ignacio-San José C. and Lillo-Ramos J., Application of electrical resistivity tomography to the environmental characterization of abandoned massive sulphide mine ponds (Iberian Pyrite Belt, SW Spain), *Near Surf. Geophys.* 8, 2010b, 65–74.

Grangeia C., Avila P., Matías M. and Ferreira Da Silva E., Mine tailings integrated investigations: the case of Rio tailings (Panasqueira Mine, Central Portugal), *Eng. Geol.* 123, 2011, 359–372.

Higuera P., Oyarzun R., Lillo J., Sánchez-Hernández J.C., Molina J.A., Esbrí J.M. and Lorenzo S., The Almaden district (Spain): anatomy of one of the world's largest Hg-contaminated sites, *Sci. Total Environ.* 356, 2006, 112–124.

Jiménez Ballesta R., Conde Bueno P., Martín Rubí J.A. and García Jiménez R., Niveles de fondo geoquímico e influencia del marco geológico en las concentraciones edafogeoquímicas de base de suelos seleccionados de Castilla-La Mancha, *Estud. Geol. Madrid* 66, 2010, 123–130.

Loke M.H. and Barker R.D., Rapid least-squares inversion of apparent resistivity pseudosections by a quasi-Newton method, *Geophys. Prospect.* 44, 1996, 131–152.

Loke M.H., Acworth I. and Dahlin T., A comparison of smooth and blocky inversion methods in 2D electrical imaging surveys, *Explor. Geophys.* 34, 2003, 182–187.

Martín-Crespo T., De Ignacio C., Gómez-Ortiz D., Martín-Velázquez S. and Lillo-Ramos F.J., Monitoring study of the mine pond reclamation of Mina Concepción, Iberian Pyrite Belt (Spain), *Environ. Earth Sci.* 59, 2010a, 1275–1284.

Martín-Crespo T., Martín-González F., Gómez-Ortiz D., Martín-Velázquez S., de Ignacio C. and Monescillo C.I., Puesta en valor del patrimonio minero dentro de itinerarios culturales: el grupo minero de San Quintín (Ciudad Real), In: Florido P. and Rábano I., (Eds.), *Una visión multidisciplinar del patrimonio geológico y minero*, 2010b, IGME; Madrid.

Martín-Crespo T., Martín-Velázquez S., Gómez-Ortiz D., de Ignacio-San José and Lillo J., A geophysical and geochemical characterization of sulphide mine ponds at the Iberian Pyrite Belt (Spain), *Water Air Soil Pollut.* 217, 2011, 287–405.

Martín-Crespo T., Gómez-Ortiz D., Martínez-Pagán P., de Ignacio-San José C., Martín-Velázquez S., Lillo J. and Faz A., Geoenvironmental characterization of riverbeds affected by mine tailings in the Mazarrón district (Spain), *J. Geochem. Explor.* 119–120, 2012, 6–16.

Martínez-Pagán P., Faz-Cano A., Arcil E. and Arocena J.M., Electrical resistivity tomography revealed the spatial chemical properties of mine tailings ponds in the Sierra Minera (SE Spain), *J. Environ. Eng. Geophys.* 14, 2009, 63–76.

Millán R., Gamarra R., Schmid T., Sierra M.J., Quejido A.J., Sánchez D.M., Cardona A.I., Fernández M. and Vera R., Mercury content in vegetation and soils of the Almadén mining area (Spain), *Sci. Total Environ.* 368, 2006, 79–87.

Montoya-Montes I., Cano-Bermejo I., Sánchez-García M.J., de Ignacio-San José C., Martín-Velázquez S., Gómez-Ortiz D., Martín-Crespo T. and Martín-González F.,

Formación de cuerpos dunares a partir de lodos mineros: mina de San Quintín (Ciudad Real, España), *Geotemas* 13, 2012, 1487–1490.

Müller G., Index of geoaccumulation in sediments of the Rhine River, *GeoJournal* 2, 1969, 108–118.

Orejas A. and Sánchez-Palencia F. J.F.J., Mines et formes de colonisation des territoires en Hispanie occidentale, In: Lévêque L., Ruiz del Árbol M., Pop L. and Bartels C., (Eds.), *Journeys through European Landscapes, [Voyages dans les paysages européens]*, 2006.

Palero F.J., Both R.A., Mangas J., Martín-Izard A. and Reguilón R., Metalogénesis de los yacimientos de Pb–Zn de la región del Valle de Alcudia (Sierra Morena Oriental), In: García Guinea J. and Martínez Frías J., (Eds.), *Recursos Minerales de*

*España*, 1992, CSIC; Madrid, 1027–1067.

Palero F.J., Both R.A., Arribas A., Boyce A.J., Mangas J. and Martín-Izard A., Geology and metallogenic evolution of the polymetallic deposits of the Alcudia Valley mineral field, Eastern Sierra Morena, Spain, *Econ. Geol.* 98, 2003, 577–605.

Pannatier Y., VarioWin - — Software for Spatial Data Analysis in 2D, 48, 1996, Springer-Verlag; New York.

Pérez-García L.C., Sánchez-Palencia F.J. and Torres-Ruiz J., Tertiary and quaternary alluvial gold deposits of Northwest Spain and Roman mining (NW of Duero and Bierzo Basins), *J. Geochem. Explor.* 71, 2000, 225–240.

Reynolds J.M., *An Introduction to Applied and Environmental Geophysics*, 1997, John Wiley and Sons; Chichester.

Rodríguez R. and Gómez J., Los residuos de la industria extractiva en España. Distribución geográfica y problemática ambiental asociada, In: Rodríguez R. and García-Cortes A., (Eds.), *Los residuos minero-metalúrgicos en el medio ambiente*, 2006, IGME; Madrid, 3–25.

Rodríguez L., Ruiz E., Alonso-Azcárate J. and Rincón J., Heavy metal distribution and chemical speciation in tailings and soils around a Pb-Zn mine in Spain, *J. Environ. Manag.* 90, 2009, 1106–1116.

Sánchez-García M.J., Lorenzo-García A., Montoya-Montes I., Martín-Velázquez S., de Ignacio-San José C., Gómez-Ortiz D., Martín-Crespo T. and Martín-González F., Transporte eólico de contaminantes en la balsa minera de San Quintín (Ciudad Real, España), *Geotemas* 13, 2012, 1499–1502.

Sasaki Y., Resolution of resistivity tomography inferred from numerical simulation, *Geophys. Prospect.* 40, 1992, 453–464.

SMMP (Société Minière et Métallurgique de Peñarroya), Libro del centenario: 1881–1981, 1981, SMMP; Ciudad Real, Spain.

Šumanovac F., Mapping of thin sandy aquifers by using high resolution reflection seismics and 2-D electrical tomography, *J. Appl. Geophys.* 58 (2), 2006, 144–157.

Sutherland R.A., Bed sediment-associated trace metals in an urban stream, Oahu, Hawaii, *Environ. Geol.* 39, 2000, 611–626.

Taylor S.R. and McLennan S.M., The geochemical evolution of the continental crust, *Rev. Geophys.* 33, 1995, 241–265, <http://dx.doi.org/10.1029/95RG00262>.

Telford W.M., Geldart L.P., Sheriff R.E. and Keys D.A., *Applied Geophysics*, 1990, Cambridge University Press; Cambridge.

US EPA, Clean Water Act, Section 503 vol. 58(no. 32), 1993, U.S. Environmental Protection Agency; Washington.

US EPA, Mercury Response Guidebook—Region 5, 2007.

US EPA, Guidelines for Water Reuse, EPA/600/R-12/618, 2012.

WHO, Air quality guidelines for Europe, WHO Regional Publications European Series 91, 2000, World Health Organization Regional Office for Europe; Copenhagen.